Research Article

Fahad Aljuaydi*, Sattam N. Almutairi, Heba Allhibi, and Abdel-Baset A. Mohamed

Nonclassical correlation dynamics of Heisenberg XYZ states with (*x*, *y*)-spin-orbit interaction, *x*-magnetic field, and intrinsic decoherence effects

https://doi.org/10.1515/phys-2025-0143 received November 15, 2024; accepted January 28, 2025

Abstract: In quantum information, it is important to recognize the effects of additional interactions, such as spin-orbit interactions, on the quantum information resources of twoqubit Heisenberg states. Therefore, we study the nonlocal correlation dynamics affected by the intrinsic decoherence of the spin-spin-Heisenberg-XYZ interaction, which is supported by spin-orbit interactions (Dzyaloshinsky-Moriya) of the x and y directions together. The two spins are coupled to an external inhomogeneous magnetic field (EIMF) in the x-direction. We investigate and compare the nonclassical correlation dynamics of local quantum Fisher information, local quantum uncertainty, and log-negativity. The results show that spin-spin and spin-orbit interactions have a high capability to enhance non-local correlations in the presence of an external magnetic field. The enhanced non-local correlation can be further improved by strengthening the spin-spin and spin-orbit interactions, as well as by increasing the EIMF's inhomogeneity and uniformity, which increases the amplitudes and fluctuations of the generated non-local correlation oscillations. The degradation of non-local correlations due to intrinsic decoherence can be controlled by spin-spin interactions. These degradation correlations can be enhanced by

increasing the intensities of spin-orbit interactions, as well as by increasing the EIMF's inhomogeneity and uniformity.

Keywords: local quantum Fisher information, magnetic field, spin–orbit interaction

1 Introduction

Among the various quantum systems proposed for implementing quantum information and computation [1,2], superconducting circuits, trapped ions, and semiconductor quantum dots are crucial techniques for realizing quantum bits (qubits). Based on electron spins trapped in quantum dots, a quantum computer protocol has been initially proposed [3-5]. The electron, having a spin of $(\frac{1}{2})$, is the simplest natural qubit. Recently, quantum computation with electron spins (as a single-spinqubit geometric gate) has been realized in quantum dots [6,7]. Due to electron tunneling from one dot to another, spin-spin coupling and spin-orbit coupling interactions between two qubits can be realized by considering a two-qubit system represented by two electrons in coupled quantum dots. Therefore, Heisenberg XYZ models describing spin-spin interactions are among the important proposed qubit systems. Two-qubit Heisenberg XYZ models have been realized in various systems, including bosonic atoms inside an optical lattice [8], trapped ions [9], superconductor systems [10], and linear molecules [11]. These models have been updated to include the first order of spin-orbit coupling known as Dzyaloshinsky-Moriya interactions [12-14], realized through an antisymmetric superexchange interaction in La₂CuO₄ [15], and the second order of spin-orbit coupling known as the Kaplan-Shekhtman-Entin-Wohlman-Aharony interaction [16]. Additionally, Heisenberg XYZ models have been updated to include dipole—dipole interactions [17] and inhomogeneous external magnetic fields [18,19]. Recently, the spin-orbit interaction was experimentally realized in two magnetic cobalt layers [20] (with Co/Ag/Co system). Moreover, the spin-orbit interaction was

Heba Allhibi: Department of Mathematical Sciences, College of Science, Princess Nourah bint Abdulrahman University, P.O. Box 84428, Riyadh, 11671, Saudi Arabia, e-mail: Haallehibi@pnu.edu.sa

Abdel-Baset A. Mohamed: Department of Mathematics, College of Science and Humanities, Prince Sattam bin Abdulaziz University, Al Kharj 11942, Saudi Arabia; Department of Mathematics, Faculty of Science, Assiut University, Assiut, Egypt

^{*} Corresponding author: Fahad Aljuaydi, Department of Mathematics, College of Science and Humanities, Prince Sattam bin Abdulaziz University, Al Kharj 11942, Saudi Arabia, e-mail: f.aljuaydi@psau.edu.sa Sattam N. Almutairi: Department of Mathematics, College of Science and Humanities, Prince Sattam bin Abdulaziz University, Al Kharj 11942, Saudi Arabia

2 — Fahad Aljuaydi et al. DE GRUYTER

experimentally implemented in the prototypical ferromagnet by polarized neutrons [21] and in ferroelectrics and antiferroelectrics [22] systems as well as in the epitaxial Ni/Cu(001) system [23]. The Heisenberg XYZ qubit models have shown several potential applications in teleportation, [24], quantum dense coding [25], thermodynamics [26], and quantum correlation generations [27].

Exploring two-qubit information dynamics in various proposed gubit systems, based on different types of nonlocal correlations (NLCs) (such as entanglement and quantum discord), is one of the most critical research fields in implementing quantum information and computation [28]. Quantum entanglement (QE), quantified by measures such as entropy [29], concurrence [30], negativity, and lognegativity [31], is a significant type of two-qubit NLCs [32,33]. It has a wide range of applications in quantum information fields, including quantum computation, teleportation [34,35], quantum optical memory [36], and quantum key distribution [37]. After implementing quantum discord as another type of qubits' NLCs beyond entanglement [38], several quantifiers have been introduced to address other NLCs [39] using Wigner-Yanase (WY) skew information [40] and quantum Fisher information (QFI) [41]. WY-skew-information minimization (local quantum uncertainty, LQU) [42] and WY-skew-information maximization (uncertaintyinduced nonlocality) [43] have been introduced to quantify other NLCs beyond entanglement. Additionally, the minimization of OFI (local quantum Fisher information, LOFI) has been used to implement another two-qubit NLC [44,45]. LQU has a direct connection to LQFI [46,47], establishing more two-gubit NLCs in several proposed gubit systems [48], such as hybrid-spin systems (under random noise [49] and intrinsic decoherence [50]), two-coupled double quantum dots [51], the mixed-spin Heisenberg model [52], and the Heisenberg system [53].

The information dynamics of two-spin Heisenberg XYZ states have been investigated using the Milburn intrinsic decoherence model [54]. This includes studies on entanglement teleportation based on the Heisenberg XYZ chain [24,55], the LQFI of Heisenberg XXX states beyond IEMF effects [56], and quantum correlations of concurrence and LQU [57]. Previous works have focused on exploring the time evolution of the two-spin Heisenberg XYZ states' NLCs under limited conditions on spin–spin and spin–orbit interactions, as well as applied magnetic fields, to ensure residing quantum information resources of two-qubit *X*-states (having an *X* density matrix) [58–62].

Motivated by the aforementioned experimental evidence for realizations for the spin-orbit interaction having a high ability to support the generating NLCs, and the importance of general two-qubit Heisenberg states, this

study employs the Milburn intrinsic decoherence and Heisenberg XYZ models to explore the NLC dynamics of LQFI, LQU, and log-negativity for general two-qubit Heisenberg XYZ states with non-X density matrices, influenced by specific conditions on spin-spin and spin-orbit interactions, as well as applied magnetic fields.

The manuscript structure includes the Milburn intrinsic decoherence equation, the Heisenberg XYZ model, and its solution in Section 2. In Section 3, we introduce the definitions of the NLCs' quantifiers: LQFI, LQU, and LN. Section 4 presents the outcomes of the dependence of these quantifiers on the physical parameters. Our conclusions are provided in Section 5.

2 Heisenberg spin model

Here, the Milburn intrinsic decoherence and Heisenberg XYZ models are used to examine the capabilities embedded in spin–spin interaction supported by the spin–orbit (Dzyaloshinsky–Moriya) interactions in the x and y directions (described by the first-order of spin–orbit couplings D_x and D_x), to generate essential NLCs between the two spin qubits under the effects of the uniformity and the inhomogeneity of an applied external inhomogeneous magnetic field (EIMF). For two spins (each described by the upper $|1_k\rangle$ and lower $|1_k\rangle$ states, where (k=A,B)), the Hamiltonian of the Heisenberg XYZ model with a spin–orbit interaction and an applied EIMF (Figure 1) is written as

$$\hat{H} = \sum_{\alpha = x,y,z} J_{\alpha} \hat{\sigma}_{A}^{\alpha} \hat{\sigma}_{B}^{\alpha} + \sum_{k = A,B} \overrightarrow{B}_{k} \cdot \overrightarrow{\sigma}_{k} + \overrightarrow{D}_{AB} \cdot (\overrightarrow{\sigma}_{A} \times \overrightarrow{\sigma}_{B}), \quad (1)$$

where $\vec{\sigma}_k = (\hat{\sigma}_k^x, \hat{\sigma}_k^y, \hat{\sigma}_k^z)$ represents the vector of Pauli matrices of the k-spin, and $\vec{B}_k = (B_k^x, B_k^y, B_k^z)$ represents the vector of the external magnetic field applying on k-spin. In our work, we consider that the EIMF is applied

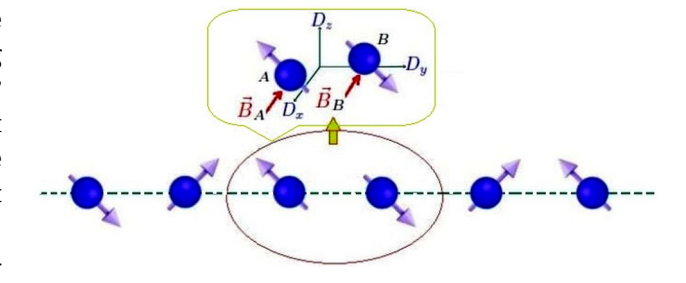


Figure 1: Diagram of a Heisenberg XYZ chain model, where two arbitrary spin–qubits (A and B) are selected with spin–orbit interaction vector $\vec{D}_{AB} = (D_x, D_y, D_z)$, and an EIMFs \vec{B}_k in the x-direction.

only in the x-direction: $\vec{B}_k = (B_k^x, 0,0), B_A^x = B_m + b_m$, and $B_{R}^{X} = B_{m} - b_{m}$. Here, B_{m} and b_{m} represent the degree of the uniformity and the inhomogeneity of the applied EIMF, respectively. For the spin-orbit interaction vector \vec{D}_{AB} = (D_x, D_y, D_z) , we have \overrightarrow{D}_{AB} . $(\overrightarrow{\sigma}_A \times \overrightarrow{\sigma}_B) = D_x \hat{C}_x + D_y \hat{C}_y + D_z \hat{C}_z$ with $\hat{C}_\alpha = \hat{\sigma}_A^{\alpha+1} \hat{\sigma}_B^{\alpha+2} - \hat{\sigma}_A^{\alpha+2} \hat{\sigma}_B^{\alpha+1} (\alpha = x, y, z)$. After considering only the spin-orbit interactions of the x and y directions $\vec{D}_{AB} = (D_x, D_y, 0)$ with an applied EIMF in the x direction, to support the spin-spin interaction in generating two-spin-qubit correlations, the considered Hamiltonian is written as

$$\hat{H} = \sum_{i=x,y,z} J_i \hat{\sigma}_A^i \hat{\sigma}_B^i + D_X (\hat{\sigma}_A^y \hat{\sigma}_B^z - \hat{\sigma}_A^z \hat{\sigma}_B^y)$$

$$+ D_y (\hat{\sigma}_A^z \hat{\sigma}_B^x - \hat{\sigma}_A^x \hat{\sigma}_B^z)$$

$$+ (B_m + b_m) \hat{\sigma}_A^x + (B_m - b_m) \hat{\sigma}_B^x.$$

$$(2)$$

In the two-spin–qubits basis: $\{|\psi_1\rangle = |1_A 1_B\rangle, |\psi_2\rangle = |1_A 0_B\rangle$, $|\psi_3\rangle = |0_A 1_B\rangle, \quad |\psi_4\rangle = |0_A 0_B\rangle\},$ the two-spin Hamiltonian in (1) can read as a non-X matrix of

$$\hat{H} = \begin{pmatrix} J_z & \beta_- & \beta_+^* & J_x - J_y \\ \beta_-^* & -J_z & J_x + J_y & \beta_+ \\ \beta_+ & J_x + J_y & -J_z & \beta_-^* \\ J_x - J_y & \beta_+^* & \beta_- & J_z \end{pmatrix}$$
(3)

with $\beta_+ = B_m \pm b_m + D_v + iD_x$. Generally, with a motion equation, this non-X Hamiltonian matrix generates twoqubit non-X states due to spin-spin interaction combined with x and y spin-orbit interactions. However, if we consider only the spin-orbit interaction in the z direction, $\vec{D} = (0, 0, D_z)$, as discussed in previous studies [58–62], the two-spin system's Hamiltonian (1) generates X-states characterized by a density X-matrix. Because deriving the analytical expressions for the eigenvalues and eigenvectors of the non-X Hamiltonian matrix (Eq. (3)) is very difficult, the eigenvalues are computed numerically.

The time evolution of the NLCs in the generated two spin-qubit states, represented by the density matrix $\hat{M}(t)$, will be explored using the Milburn intrinsic decoherence model [54], which is given by

$$\frac{d}{dt}\hat{M}(t) = -i[\hat{H}, \hat{M}] - \frac{\gamma}{2}[\hat{H}, [\hat{H}, \hat{M}]], \tag{4}$$

where γ is the intrinsic spin–spin decoherence (ISSD) coupling.

After calculating the eigenvalues V_k (k = 1, 2, 3, 4) and the eigenstates $|V_k\rangle$ of the Hamiltonian in Eq. (3), the twospin density matrix $\hat{M}(t)$ of Eq. (4) can be obtained numerically using the following solution, given by

$$\hat{M}(t) = \sum_{m,n=1}^{4} U_{mn}(t) S_{mn}(t) \langle V_m | \hat{M}(0) | V_n \rangle | V_m \rangle \langle V_n |.$$
 (5)

This solution depends on the unitary interaction $U_{mn}(t)$ and the ISSD coupling $S_{mn}(t)$, given by the following terms:

$$U_{mn}(t) = e^{-i(V_m - V_n)t},$$

$$S_{mn}(t) = e^{-\frac{y}{2}(V_m - V_n)^2 t}.$$
(6)

Eq. (5) is used to numerically calculate and explore the dynamics of the NLCs within the two-spin-qubit states' Heisenberg XYZ model under the effects of spin-orbit interactions along the x and y directions and an applied external magnetic field in the x direction.

3 NLC quantifiers

Here, the two-spin NLCs will be measured by the following quantifiers: LQFI, LQU, and LN.

LOFI

Here, we use LQFI to quantify another type of two-spin Heisenberg-XYZ correlation beyond entanglement. After calculating the two-spin eigenvalues π_k (k = 1, 2, 3, 4) and the eigenstates $|\Pi_k\rangle$ of the density matrix of Eq. (5), which has the representation matrix $M(t) = \sum_{m} \pi_{m} |\Pi_{m}\rangle \langle \Pi_{m}|$ with $\pi_m \ge 0$ and $\sum_m \pi_m = 1$, the LQFI is calculated using the closed expression given by [41,44,45]

$$F(t) = 1 - \pi_R^{\max},$$

which depends on the highest eigenvalue π_R^{\max} of the symmetric matrix $R = [r_{ij}]$. Based on the Pauli spin- $\frac{1}{2}$ matrices σ^i (i = 1, 2, 3) and the elements $\xi^i_{mn} = \langle \Pi_m | I \otimes \sigma^i | \Pi_n \rangle$, the symmetric matrix elements r_{ii} are given by

$$r_{ij} = \sum_{\pi_m + \pi_n \neq 0} \frac{2\pi_m \pi_n}{\pi_m + \pi_n} \xi_{mn}^i (\xi_{nm}^j)^{\dagger}.$$

For a maximally correlated two-spin-qubit state, the LQFI function converges to F(t) = 1. Otherwise, the LQFI function oscillates and is bounded by the inequality 0 < F(t) < 1, indicating that the states have partial LOFI NLC.

• LQU

Also, we use LQU of WY skew information [40] to realize another type of two-spin-qubits' NLC [40,42,43]. For the two-spin density matrix M(t) of Eq. (5), the LQU can be calculated by the following closed expression [42]:

$$U(t) = 1 - \lambda_{\max}(\Lambda_{AB}), \tag{7}$$

which depends on the largest eigenvalue λ_{max} of the 3×3 -matrix $\Lambda = [a_{ij}]$, which have the following elements:

$$a_{ii} = \operatorname{Tr}\{\sqrt{M(t)}(\sigma_i \otimes I)\sqrt{M(t)}(\sigma_i \otimes I)\}.$$

4 — Fahad Aljuaydi et al. DE GRUYTER

The LQU function oscillates and is bounded by the inequality $0 \le U(t) \le 1$. It converges to U(t) = 1, otherwise indicating that the states have partial LQU NLC.

· Logarithmic negativity (LN)

We employ LN [31] to measure the generated two-spin–qubit entanglement. The LN expression is based on the negativity's definition μ_t , which is defined as the absolute sum of the negative eigenvalues of the partial transposition matrix $(M(t))^T$ of the two-spin–qubit density matrix M(t) of Eq. (5). The LN can be expressed as

$$N(t) = \log_2[1 + 2\mu_t]. \tag{8}$$

The LN function vanishes, N(t)=0, for a disentangled two-spin state. It converges to its maximum value, N(t)=1, for a maximally entangled two-spin state. Otherwise, LN oscillates and is bounded by the inequality $0 \le N(t) \le 1$, indicating that the two-spin states have partial entanglement.

In the following, we work in a system of units where $\hbar=1$, and employ the nondimensionalized parameter method as described in previous studies [24,63,64]. We also consider the case of spin–spin interactions with antiferromagnetic couplings satisfying $J_{\alpha}>0$. Meanwhile, the other physical parameters, including the spin–orbit couplings and the degree of uniformity and inhomogeneity of the magnetic field, satisfy D_x , D_y , B_m , $b_m \ge 0$. Small values of these parameters indicate weak spin–orbit interaction and a weak applied magnetic field.

4 Two-spin qubit dynamics

To explore the generation of non-local correlations between two spin qubits, we consider that the two spins are initially in their uncorrelated upper states $|1_A\rangle \otimes |1_B\rangle$. In this state, the density matrix has no non-local correlations according to the considered quantifiers. Our focus is on the effects of J_a spin–spin interactions (D_x and D_y) and inhomogeneous x-direction magnetic field parameters (B_m and D_m) in the presence of ISSD coupling.

Our first analysis, starting from Figure 2, illustrates the dynamics of non-local correlations (LQFI, LQU, and LN) between two spin qubits. These correlations are generated by the couplings $(J_x, J_y, J_z) = (0.8, 0.8, 0.8)$, supported by varying intensities of x and y spin-orbit interactions. This is done in the presence of an inhomogeneous x-direction magnetic field with small uniformity and inhomogeneity $(B_m, b_m) = (0.3, 0.5)$, and in the absence of intrinsic spin-spin decoherence (y = 0). Figure 2(a) with $(D_x, D_y) = (0.5, 0.5)$

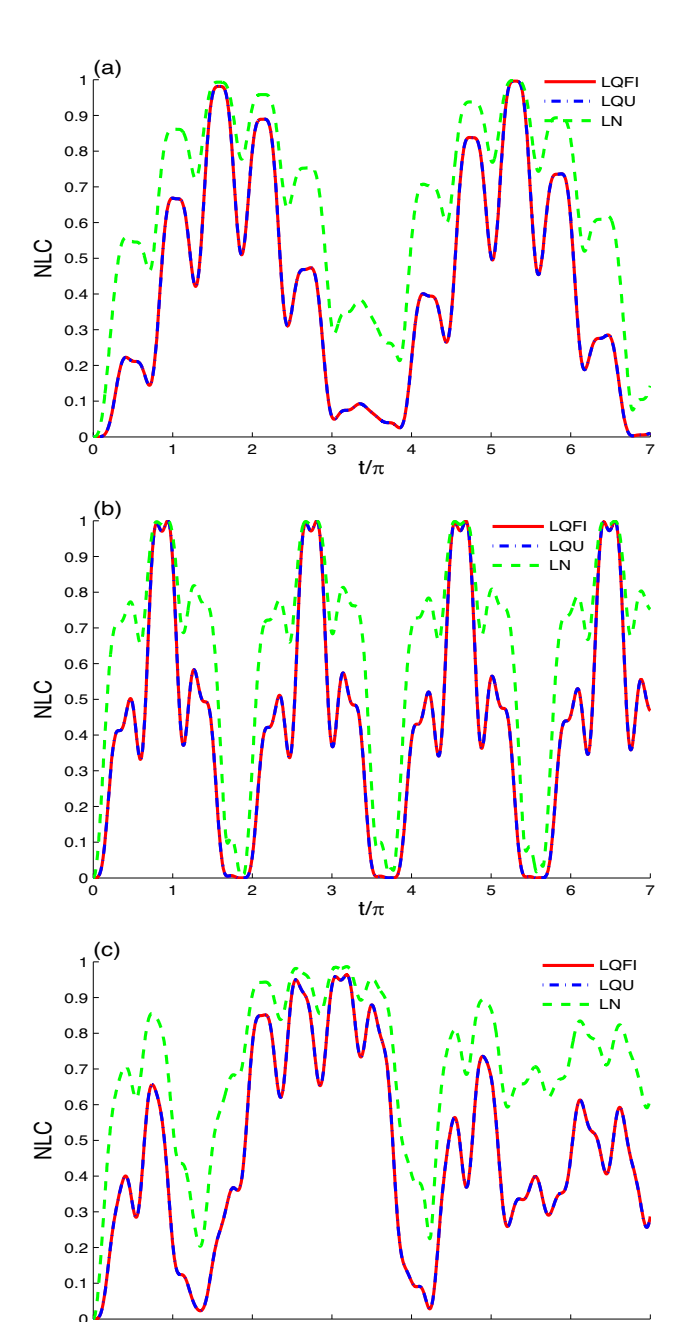


Figure 2: Time evolution of the LQFI, LQU, and LN are shown with the two-spin couplings $(J_x, J_y, J_z) = (0.8, 0.8, 0.8)$ and the applied magnetic field parameters $(B_m, b_m) = (0.3, 0.5)$ for different x, y spin–orbit interactions: $(D_x, D_y) = (0.0, 0.0)$ in (a), $(D_x, D_y) = (0.5, 0.0)$ in (b), and $(D_x, D_y) = (0.5, 0.5)$ in (c).

t/π

(0.0, 0.0) shows that the LQFI, LQU, and log-negativity grow and reach their maximum values. They are subject to slow quasi-regular oscillations with the same frequencies and different amplitudes. LQFI and LQU have the same behavior, i.e., the two spin qubit correlation is called "LQFI-LQU correlation." The amplitude of the LN is always

larger than that of the LQFI and LQU. Under these circumstances of a weak coupling regime ($J_a = 0.8$) and the applied inhomogeneous x-direction magnetic field (with weak uniformity and inhomogeneity), the initial pure uncorrelated twospin state evolves into various time-dependent partially correlated states. At specific times, it transforms into maximally correlated states. The two-spin states exhibit maximal LQFI–LQU correlation (F(t) = U(t) = 1) and log-negativity (N(t) = 1) simultaneously. At particular times, we observe that partially entangled two-spin states have neither LQFI nor LQU correlation.

The D_x -spin-orbit interaction $(D_x, D_y) = (0.5, 0)$ dramatically improves the appearance of the intervals of the maximal LOFI-LOU correlation and log-negativity entanglement, as well as the intervals in which two-spin entangled states have no LQFI or LQU correlation. The effects of weak spin-orbit interactions in the x direction only are shown in Figure 2(b). As illustrated, the regularity and fluctuations of the generated LQFI-LQU correlation and log-negativity entanglement are significantly greater than previously observed in the absence of x and y spin-orbit interactions. The weak D_x spin-orbit interaction dramatically enhances the intervals of maximal LOFI-LOU correlation and log-negativity entanglement, as well as the intervals where two-spin entangled states have neither LQFI nor LQU correlation. In Figure 2(c), we combined the D_x and D_y spin-orbit interactions $(D_x, D_y) = (0.5, 0.5)$. As shown, the fluctuations of the two-spin NLCs between their partial and maximal values are significantly fewer than in Figure 2(a) and (b). Additionally, the NLC frequencies have been reduced, and their lower bounds have shifted upward. This indicates that the combined D_x and D_y spin-orbit interactions enhance the generated partial two-spin-qubit LQFI-LQU correlation and log-negativity entanglement.

Figure 3(a) and (b) illustrates that higher spin-spin interaction couplings $((J_x, J_y, J_z) = (1, 0.5, 1.5)$ in (a) and (J_x, J_y, J_z) = (5, 1, 1.5) in (b)) significantly enhance the twospin LQFI-LQU correlation and log-negativity entanglement. By comparing the generated spin-spin NLCs shown in Figur 2(c) and 3(a), we find that relatively strong couplings of J_q -spin–spin interactions $((J_x, J_y, J_z) = (1, 0.5, 1.5))$, supported by weak $D_{x,y}$ -spin-orbit interactions ((D_x, D_y) = (0.5, 0.5)), increase the amplitudes and frequencies of the LQFI-LQU correlation and log-negativity entanglement oscillations. Figure 3(a) and (b) shows that higher I_a -couplings lead to that the spin-spin NLCs' oscillations have more fluctuations. The time positions of the maximal LQFI-LQU correlation and log-negativity entanglement are enhanced. Figure 3(c) is plotted to demonstrate the capability of spin–spin interactions ($J_a = 0.8$), supported

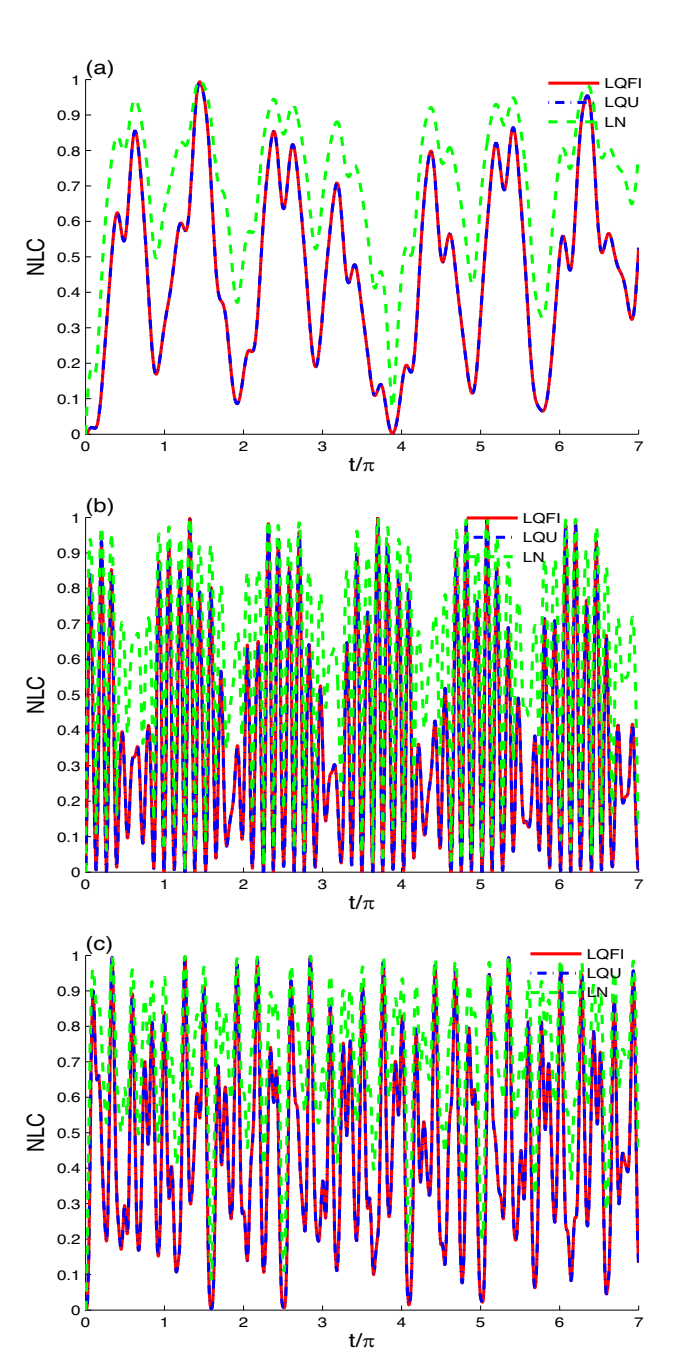


Figure 3: Time evolution of the LQFI, LQU, and LN of Figure 2(c) are plotted for different two-spin couplings: $(J_x, J_y, J_z) = (1, 0.5, 1.5)$ in (a) and (J_x, J_y, J_z) = (5, 1, 1.5) in (b). In (c), they are plotted for x, y spin-orbit couplings $D_x = D_y = 2$ in (c).

by x, y-spin-orbit interactions ($D_x = D_y = 2$), to enhance the generated spin-spin NLCs when an external magnetic field with weak determinants $((B_m, b_m) = (0.3, 0.5))$ is applied. By comparing the qualitative dynamics of the generated LQFI-LQU correlation and log-negativity entanglement shown in Figure 2(c) ($D_x = D_y = 0.5$) with those in Figure 3(c) $(D_x = D_y = 2)$, we can deduce that $D_{x,y}$ -spin—orbit interactions play a significant role in enhancing the generated LQFI-LQU correlation and lognegativity entanglement. Their amplitudes are increased, and their oscillations exhibit more fluctuations between extreme values. Additionally, strong x, y-spin—orbit interactions potentially strengthen and accelerate the generation of LQFI—LQU correlation and log-negativity entanglement due to J_a -spin—spin interactions.

Figure 4 illustrates the LQFI–LQU correlation and lognegativity entanglement dynamics of Figure 3(a) (where (J_x,J_y,J_z) = (1, 0.5, 1.5), b_m = 0.5, and D_x = D_y = 0.5) for different uniformities of the applied EIMF. Figure 4(a) illustrates that with a large uniformity (B_f = 2), increasing the EIMF uniformity delays the growth of LQFI, LQU, and lognegativity. It also increases the fluctuations of the two-spin state between different partially and maximally correlated states. The generations of the LQFI–LQU correlation and log-negativity entanglement are shown in Figure 4(b) (with B_m = 10), confirming that increasing the EIMF uniformity enhances the ability of strong J_α -spin—spin interactions, supported by weak x, y-spin—orbit interactions, to create partially and maximally correlated states with greater

stability. However, the generated spin–spin NLCs become more sensitive to the EIMF uniformity.

In the upcoming analysis of Figure 5, we maintain the same parameter values as in Figure 3a (with (J_x, J_y, J_z) = $(1, 0.5, 1.5), B_m = 0.3, \text{ and } D_x = D_y = 0.5)$ and examine different magnetic field inhomogeneities: $b_m = 2$ in (a) and $b_m = 10$ in (b). In the case of Figure 5(a), we observe that greater EIMF uniformities improve the efficiency of generating LQFI-LQU correlations and log-negativity entanglement. The uniformity of the EIMF increases the fluctuations of the two-spin state between different partially and maximally correlated states. The timing of the maxima $(F(t) = U(t) = N(t) \approx 1)$ and minima (zero-value) ($F(t) = U(t) = N(t) \approx 0$) of the generated LQFI-LQU correlations and log-negativity entanglement is enhanced. Figure 5(b) demonstrates that an increase in EIMF inhomogeneity significantly enhances the generated two-spin-qubits' NLCs, leading to greater amplitudes and fluctuations in the NLC oscillations.

The next illustrations in Figures 6–8 depict the time evolutions of NLCs of LQFI, LQU, and log-negativity in the presence of non-zero ISSD coupling. By comparing the results of Figure 2(a) (y = 0.0) with those of Figure 6(a)

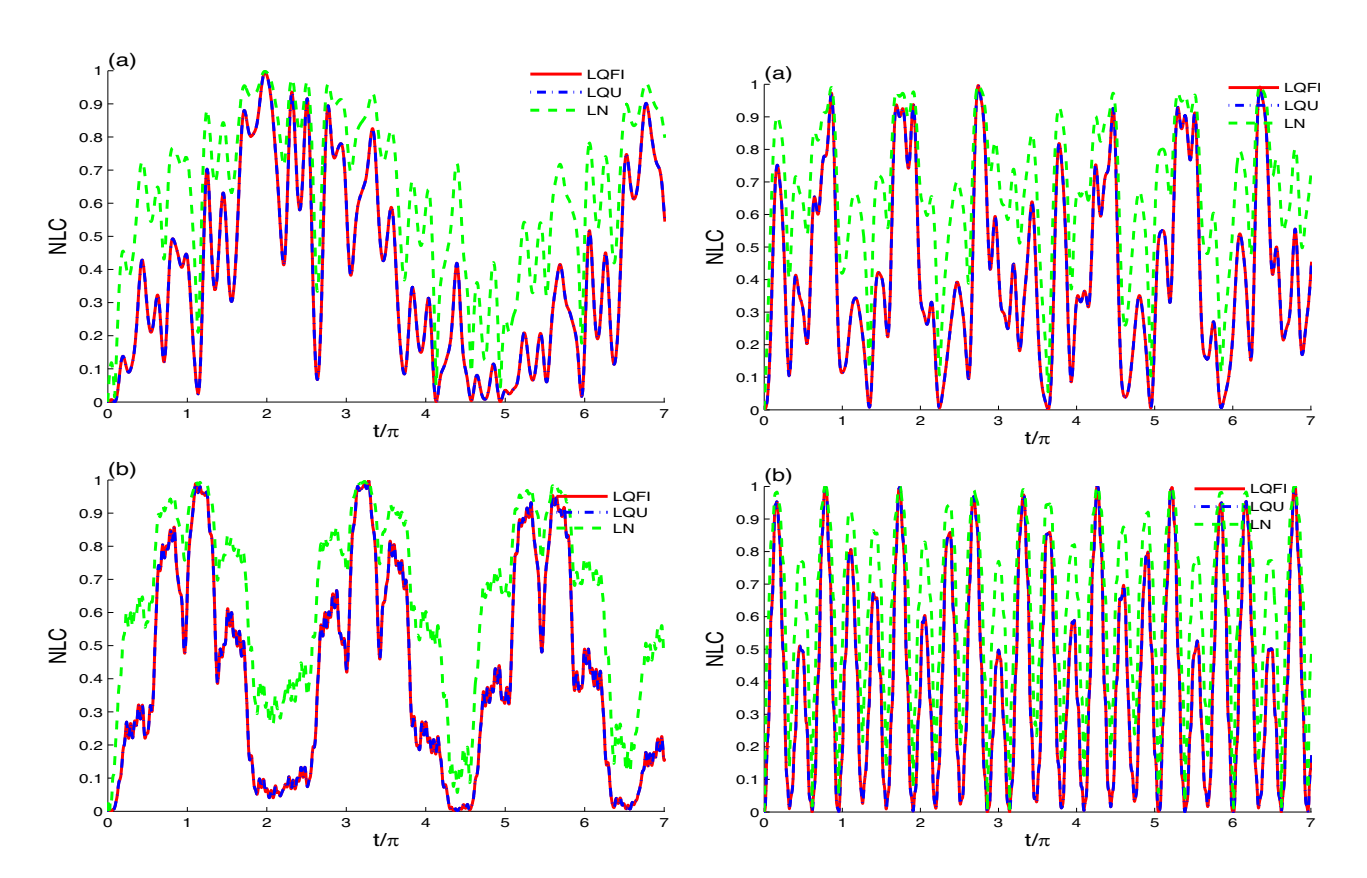


Figure 4: Time evolutions of LQFI, LQU, and LN of Figure 3(a) (for (J_x,J_y,J_z) = (1, 0.5, 1.5), b_m = 0.5, and D_x = D_y = 0.5) are plotted for different EIMF uniformities: B_m = 2 in (a) and B_m = 10 in (b).

Figure 5: Time evolutions of LQFI, LQU, and LN of Figure 3(a) (for (J_x, J_y, J_z) = (1, 0.5, 1.5), B_m = 0.3, and D_x = D_y = 0.5) are plotted for different EIMF inhomogeneities: b_m = 2 in (a) and b_m = 10 in (b).

 $(\gamma=0.05)$, we observe that LQFI, LQU, and log-negativity exhibit different decaying oscillatory dynamical evolutions. The generations of Heisenberg-XYZ states' NLCs, due to $J_{\alpha}=0.8$ spin–spin couplings and the applied magnetic field $(B_m,b_m)=(0.3,0.5)$ without spin–orbit interaction, are weakened and exhibit different amplitudes, which decrease with increasing ISSD coupling. After a certain time interval, with non-zero ISSD coupling, LQFI and LQU show different NLCs with varying amplitudes but

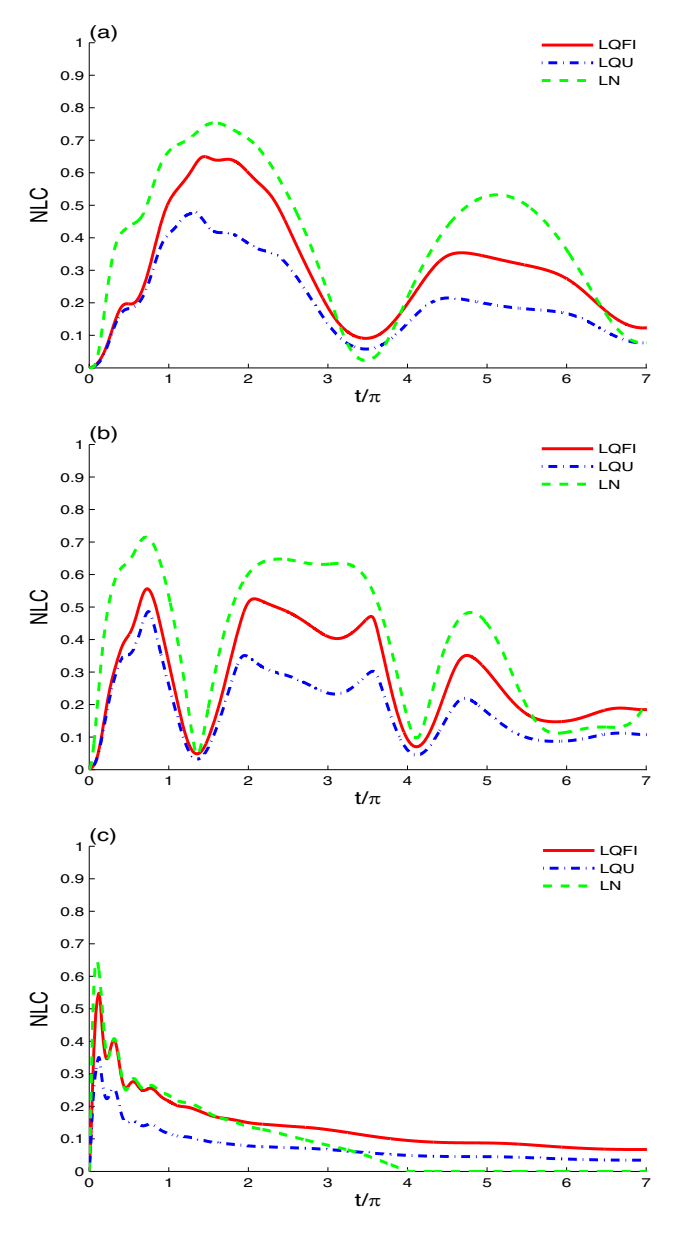


Figure 6: Time evolutions of LQFI, LQU, and LN of Figure 2(a) are shown in the presence of the ISSD effect ($\gamma=0.05$) with EIMF uniformity and inhomogeneity (B_m , b_m) = (0.3, 0.5), and two-spin couplings $J_\alpha=0.8$ for different couplings: $D_k=0$ (k=x,y) in (a), $D_k=0.5$ in (b), and $D_k=2$ in (c).

similar behaviors. Moreover, the robustness of LQFI and log-negativity against the ISSD effect is greater for LQU.

As shown in Figure 6(b) and (c), increasing the intensities of x, y-spin-orbit interactions reduces the robustness of NLCs against the ISSD effect. The amplitudes of NLCs significantly decrease as the x, y-spin-orbit interactions increase. Moreover, LQFI and LQU exhibit sudden changes at different times. The phenomenon of sudden changes has been studied both theoretically [65] and experimentally [66]. For very strong x, y-spin—orbit interactions ($D_k = 2$) Figure 6(c), we observe that the log-negativity of the twospin qubit drops instantly to zero at a specific time and remains zero for an extended period (i.e., the sudden-death LN-entanglement phenomenon occurs). After this, the disentangled two-spin states exhibit only different stable NLCs of LQFI and LQU. We can conclude that the decay of NLCs due to ISSD can be intensified by increasing the intensities of x, y-spin-orbit interactions.

Figure 7 illustrates the time evolutions of LQFI, LQU, and LN of Figure 6(b) and (c), but for strong spin–spin couplings with $(J_x, J_y, J_z) = (1, 0.5, 1.5)$. By comparing Figures 6(b), (c) and 7(a), (b), we find that strong spin–spin couplings $(J_x, J_y, J_z) = (1, 0.5, 1.5)$ reduce the ISSD effect and

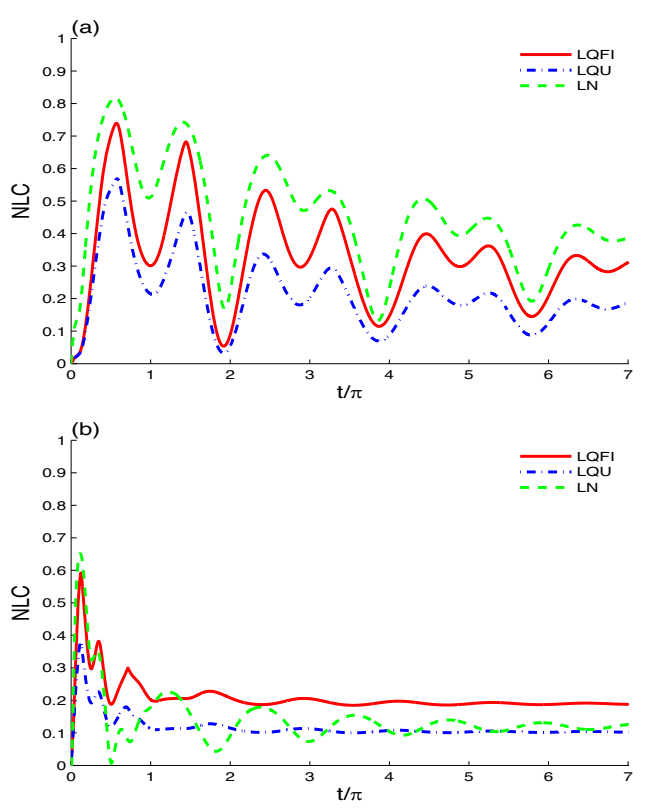


Figure 7: Time evolutions of LQFI, LQU, and LN of Figure 6(b) and (c) are shown but for strong spin–spin couplings with (J_x, J_y, J_z) = (1, 0.5, 1.5).

8 — Fahad Aljuaydi et al. DE GRUYTER

improve the robustness of the NLCs (against the ISSD effect) of LQFI, LQU, and LN. For very strong spin–orbit interactions $D_k=2$ (Figure 7(b)), the sudden-death LN-entanglement phenomenon does not occur, except instantaneously at $t\approx 0.5\pi$. The generated two-spin states have different stable partial NLCs of LQFI, LQU, and LN. In this case, the decay of NLCs due to ISSD can be mitigated by enhancing the spin–spin interactions.

Figure 8(a) shows the time evolutions of LQFI, LQU, and LN from Figure 4(a) for $(J_x, J_y, J_z) = (1, 0.5, 1.5)$ and $D_x = D_y = 0.5$, considering the ISSD effect (y = 0.05) after strengthening the EIMF uniformity with $(B_m, b_m) = (2, 0.5)$. In this case, we observe that the large EIMF uniformity $B_m = 2$ increases the NLCs' decay resulting from ISSD. Time intervals appear in which the disentangled two-spin states have only different stable NLCs of LQFI and LQU. Moreover, the robustness of LQFI and LN NLCs, against the ISSD effect, is reduced by increasing EIMF uniformity. The results shown in Figure 8(b) demonstrate that increasing the inhomogeneity of the EIMF to $b_m = 2$ enhances the degradation of the NLC functions. Under the parameters $b_m = 2$, $(J_x, J_y, J_z) = (1, 0.5, 1.5)$, and $D_k = 0.5$, we observe

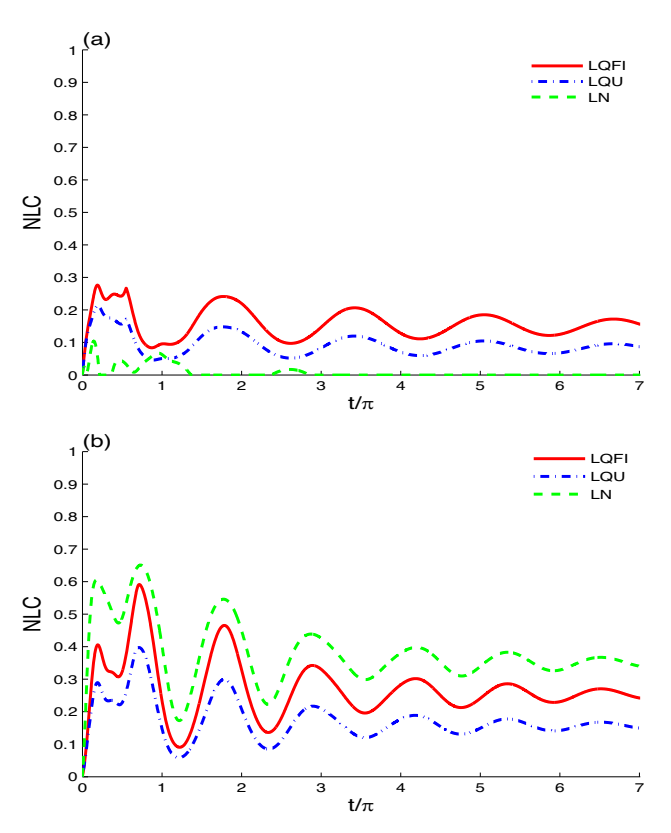


Figure 8: Time evolutions of LQFI, LQU, and LN in Figure 4(a), for $(J_x, J_y, J_z) = (1, 0.5, 1.5)$ and $D_x = D_y = 0.5$, are presented considering the ISSD effect $(\gamma = 0.05)$ for EIMF uniformity with $(B_m, b_m) = (2, 0.5)$ in (a) and EIMF inhomogeneity with $(B_m, b_m) = (0.3, 2)$ in (b).

that the generated NLCs (LQFI, LQU, and entanglement) in Figure 4(a) degrade (due to the ISSD effect) and quickly reach their partially stable oscillatory behaviors, compared to the case with a small value of b_m = 0.5 in Figure 7(a). We find that the EIMF's inhomogeneity has a lesser ability to enhance the ISSD effect compared to its uniformity.

5 Conclusion

In this study, we use the Milburn intrinsic decoherence and the Heisenberg XYZ models to explore the capabilities of spin-spin and spin-orbit interactions (in the x and y directions) to generate NLCs (measured by LQFI, LQU, and LN) under the influence of the uniformity and inhomogeneity of the EIMF in the x direction. The generated NLCs are examined in the absence of the ISSD, as the parameters of spin-spin and spin-orbit interactions, as well as the EIMF's uniformity and inhomogeneity, are increased. It is found that the spin-spin Heisenberg XYZ and x, y-spinorbit interactions have a strong ability to enhance non-local correlations with small external magnetic field parameters. The spin-orbit interactions significantly contribute to the enhancement of the generated two-spin-qubits LQFI-LQU correlation and log-negativity entanglement, increasing their oscillation amplitudes and fluctuations. In the presence the ISSD, the generation of NLCs is weakened and exhibits varying amplitudes, decreasing as the ISSD coupling increases. The robustness of LQFI and log-negativity against the ISSD effect is greater than that of LQU. Sudden changes occur during the dynamics of LQU and LQFI, while sudden death occurs during the dynamics of log-negativity entanglement. The decay of NLCs due to ISSD can be enhanced by increasing the intensities of x, y-spin-orbit interactions. Strengthening the spin-spin interactions, however, weakens the NLCs' decay resulting from ISSD. The generated NLCs degrade quickly due to the ISSD effect with a large IMF's inhomogeneity, reaching their partially stable oscillatory behaviors. The ability of the IMF's inhomogeneity to increase the ISSD effect is small compared to that of the EIMF's uniformity. Our findings on the generated two-spin qubit NLCs (measured by LQFI, LQU, and LN) resulting from spin-spin interactions, supported by spin-orbit interactions in the x and y directions and an applied EIMF in the x direction, pave the way for exploring other quantum effects with the considered interaction directions or with different interaction directions. Additionally, these quantum effects can be explored using other differential motion equations with the considered interaction directions.

Furthermore. fractional quantum calculus Riemann-Liouville integration [67,68] can be employed to investigate fractional quantum phenomena in the considered Heisenberg XYZ model using fractional differential motion equations [69,70].

Acknowledgments: The author is very grateful to the referees and the associate editor for their important remarks which have helped him to improve the manuscript. This study is supported via funding from Prince sattam bin Abdulaziz University Project Number (PSAU/ 2025/R/1446).

Funding information: This study was funded by Princess Nourah bint Abdulrahman University Researchers Supporting Project Number (PNURSP2025R906), Princess Nourah bint Abdulrahman University, Riyadh, Saudi, Arabia.

Author contributions: Sattam N. Almutairi, Heba Allhibi, and Fahad Aljuaydi prepared all the figures and performed the mathematical calculations. Heba Allhibi, Sattam N. Almutairi, and Fahad Aljuaydi wrote the original draft. Abdel-Baset A. Mohamed, Sattam N. Almutairi, and Fahad Aljuaydi reviewed and edited the draft. All authors have accepted responsibility for the entire content of this manuscript and approved its submission.

Conflict of interest: The authors state no conflict of interest.

Data availability statement: The datasets generated during and/or analysed during the current study are available from the corresponding author on reasonable request.

References

- Horodecki R, Horodecki P, Horodecki M, Horodecki K. Quantum entanglement. Rev Mod Phys. 2009;81:865.
- Nielsen MA, Chuang IL. Quantum computation and quantum information. Cambridge: Cambridge University Press; 2000.
- Loss D, DiVincenzo DP. Quantum computation with quantum dots. Phys Rev A 1998;57:120.
- Burkard G, Loss D, DiVincenzo DP. Coupled quantum dots as quantum gates. Phys Rev B. 1999;59:2070.
- Vandersypen LMK, Hanson R, van Willems Beveren LH, Elzerman JM, Greidanus JS, De Franceschi S, et al. Quantum computing and quantum bits in mesoscopic systems. Boston, M A.: Springer; 2004.
- Ma R-L, Li A-R, Wang C, Kong ZZ, Liao W-Z, Ni M, et al. Singlespin-qubit geometric gate in a silicon quantum dot. Phys Rev Appl. 2024;21:014044.
- Zwolak JP, Taylor JM. Colloquium: Advances in automation of quantum dot devices control. Rev Mod Phys. 2023;95:011006.

- Pinheiro F, Bruun GM, Martikainen J-P, Larson J. XYZ Quantum Heisenberg Models with p-Orbital Bosons. Phys Rev Lett. 2013;111:205302.
- Bermudez A, Tagliacozzo L, Sierra G, Richerme P. Long-range [9] Heisenberg models in quasiperiodically driven crystals of trapped ions. Phys Rev B Condens Matter Mater Phys. 2017;95:024431.
- Nishiyama M, Inada Y, Zheng GQ. Spin triplet superconducting state due to broken inversion symmetry in Li₂Pt₃B. Phys Rev Lett. 2007;98:047002.
- [11] Yue W, Wei Q, Kais S, Friedrichc B, Herschbach D. Realization of Heisenberg models of spin systems with polar molecules in pendular states. Phys Chem Chem Phys. 2022;24:25270.
- Dzyaloshinski I. A thermodynamic theory of "weak" ferromagnetism of antiferromagnetics, I Phys Chem Solids, 1958:4:241.
- Moriya T. Theory of Magnetism of NiF2. Phys Rev. 1960;117:635. [13]
- Moriya T. New mechanism of anisotropic superexchange interaction. Phys Rev Lett. 1960;4:228.
- [15] Shekhtman L, Entin-Wohlman O, Aharony A. Bond-dependent symmetric and antisymmetric superexchange interactions in La₂CuO₄. Phys Rev B. 1993;47:174.
- Moriya T. Anisotropic superexchange interaction and weak Ferromagnetism. Phys Rev. 1960;120:91.
- Kuznetsova EI, Yurischev MA. Quantum discord in spin systems [17] with dipole-dipole interaction. Quantum Inf Process. 2013;12:3587-605.
- Arnesen MC, Bose S, Vedral V. Natural thermal and magnetic entanglement in the 1D Heisenberg model. Phys Rev Lett. 2001;87:017901.
- [19] Li D-C, Cao Z-L. Thermal entanglement in the anisotropic Heisenberg (XYZ) model with different inhomogeneous magnetic fields. Optics Commun. 2009;282:1226-30.
- Matthies T, Rózsa L, Szunyogh L, Wiesendanger R, Vedmedenko EY. Interlayer and interfacial Dzyaloshinskii-Moriya interaction in magnetic trilayers: First-principles calculations. Phys Rev Res. 2024;6:043158.
- [21] Thoma H, Hutanu V, Deng H, Dmitrienko VE, Brown PJ, Gukasov A, et al. Revealing the absolute direction of the Dzyaloshinskii-Moriya interaction in prototypical weak ferromagnets by polarized neutrons. Phys Rev X. 2021;11:011060.
- [22] Zhao HJ, Chen P, Prosandeev S, Artyukhin S, Bellaiche L. Dzyaloshinskii-Moriya-like interaction in ferroelectrics and antiferroelectrics. Nature Materials. 2021;20:341.
- [23] Allenspach R, Bischof A, Boehm B, Drechsler U, Reich O, Sousa M, et al. Dzyaloshinskii-Moriya interaction in Ni/Cu(001). Phys Rev B. 2024;110:014402.
- [24] Hosseiny SM, Seyed-Yazdi J, Norouzi M, Livreri P. Quantum teleportation in Heisenberg chain with magnetic-field gradient under intrinsic decoherence. Sci Rep. 2024;14:9607.
- [25] Khedif Y, Muthuganesan R. Intrinsic decoherence dynamics and dense coding in dipolar spin system. Appl Phys B. 2023;129:19.
- Abd-Rabbou MY, ur Rahman A, Yurischev MA, Haddadi S. Comparative study of quantum Otto and Carnot engines powered by a spin working substance. Phys Rev E. 2023;108:034106.
- Yurischev MA. On the quantum correlations in two-qubit XYZ spin [27] chains with Dzyaloshinsky-Moriya and Kaplan-Shekhtman-Entin-Wohlman-Aharony interactions. Quantum Inf Process.
- [28] Le Bellac M. A short introduction to quantum information and quantum computation. Cambridge: Cambridge University Press; 2006.

- [29] Eisert J, Cramer M, Plenio MB. Colloquium: Area laws for the entanglement entropy. Rev Mod Phys. 2010;82:277.
- [30] Wootters WK. Entanglement of formation of an arbitrary state of two qubits. Phys Rev Lett. 1998;80:2245.
- [31] Vidal G, Werner RF. Computable measure of entanglement. Phys Rev A. 2002;65:032314.
- [32] Eftekhari F, Tavassoly MK, Behjat A, Faghihi MJ. Entanglement and atomic inversion in a dissipative two-atom-optomechanical system. Optics Laser Tech. 2024;168:109934.
- [33] Abdel-Wahab NH, Zangi SM, Seoudy TA, Haddadi S. Dynamical evolution of a five-level atom interacting with an intensity-dependent coupling regime influenced by a nonlinear Kerr-like medium. Sci Rep. 2024;14:25211.
- [34] Braunstein SL, Kimble HJ. Teleportation of continuous quantum variables. Phys Rev Lett. 1998;80:869.
- [35] Bouwmeester D, Pan JW, Mattle K, Eibl M, Weinfurter H, Zeilinger A. Experimental quantum teleportation. Nature. 1997;390:575.
- [36] Lei Y, Asadi FK, Zhong T, Kuzmich A, Simon C, Hosseini M. Quantum optical memory for entanglement distribution. Optica. 2023;10:1511–28.
- [37] Ekert AK. Quantum cryptography based on Bell's theorem. Phys Rev Lett. 1991:67:661.
- [38] Ollivier H, Zurek WH. Quantum discord: A measure of the quantumness of correlations. Phys Rev Lett. 2001;88:017901.
- [39] Hu M-L, Hu X, Wang J, Peng Y, Zhang Y-R, Fan H. Quantum coherence and geometric quantum discord. Phys Rep. 2018;762:1.
- [40] Wigner EP, Yanase MM. Information contents of distributions. Proc Natl Acad Sci. 1963;49:910.
- [41] Girolami D, Souza AM, Giovannetti V, Tufarelli T, Filgueiras JG, Sarthour RS, et al. Quantum discord determines the interferometric power of quantum states. Phys Rev Lett. 2014:112:210401
- [42] Girolami D, Tufarelli T, Adesso G. Characterizing nonclassical correlations via local quantum uncertainty. Phys Rev Lett. 2013:110:240402.
- [43] Wu S-X, Zhang J, Yuuu C-S, Song H-S. Uncertainty-induced quantum nonlocality. Phys Lett A. 2014;378:344.
- [44] Dhar HS, Bera MN, Adesso G. Characterizing non-Markovianity via quantum interferometric power. Phys Rev A. 2015;991:032115.
- [45] Kim S, Li L, Kumar A, Wu J. Characterizing nonclassical correlations via local quantum Fisher information. Phys Rev A. 2018;97:032326.
- [46] Helstrom CW. Quantum detection and estimation theory. New York: Academic; 1976.
- [47] Paris MGA. Quantum estimation for quantum technology. Int J Quant Inf. 2009;7:125.
- [48] Mohamed A-B A, Farouk A, Yassen MF, Eleuch H. Fisher and skew information correlations of two coupled trapped ions: Intrinsic decoherence and Lamb-Dicke nonlinearity. Symmetry. 2021;13:2243.
- [49] Benabdallah F, Ur Rahman A, Haddadi S, Daoud M. Long-time protection of thermal correlations in a hybrid-spin system under random telegraph noise. Phys Rev E. 2022;106:034122.
- [50] Benabdallah F, El Anouz K, Ur Rahman A, Daoud M, El Allati A, Haddadi S. Witnessing quantum correlations in a hybrid Qubit-Qutrit system under intrinsic decoherence. Fortschr Phys. 2023;71:2300032.
- [51] Elghaayda S, Dahbi Z, Mansour M. Local quantum uncertainty and local quantum Fisher information in two-coupled double quantum dots. Opt Quant Electron 2022;54:419.

- [52] Wei P-F, Luo Q, Wang H-Q-C, Xiong S-J, Liu B, Sun Z. Local quantum Fisher information and quantum correlation in the mixed-spin Heisenberg XXZ chain. Front Phys. 2024;19:21201.
- [53] Fedorova AV, Yurischev MA. Behavior of quantum discord, local quantum uncertainty, and local quantum Fisher information in two-spin-1/2 Heisenberg chain with DM and KSEA interactions. Quantum Inf Process. 2022;21:92.
- [54] Milburn GJ. Intrinsic decoherence in quantum mechanics. Phys Rev A. 1991;44:5401.
- [55] Qin M, Ren Z-Z. Influence of intrinsic decoherence on entanglement teleportation via a Heisenberg XYZ model with different Dzyaloshinskii-Moriya interactions. Quantum Inf Process. 2015;14:2055–66.
- [56] Mohamed A-B A, Aldosari FM, Eleuch H. Two-qubit-Heisenberg local quantum Fisher information dynamics induced by intrinsic decoherence model. Results Phys. 2023;49:106470.
- [57] Ait Chlih A, Habiballah N, Nassik M. Dynamics of quantum correlations under intrinsic decoherence in a Heisenberg spin chain model with Dzyaloshinskii–Moriya interaction. Quantum Inf Process. 2021;20:92.
- [58] Jafari R, Akbari A. Dynamics of quantum coherence and quantum Fisher information after a sudden quench. Phys Rev A. 2020;101:062105.
- [59] Mo C, Zhang G-F. The effect of acceleration parameter on thermal entanglement and teleportation of a two-qubit Heisenberg XXX model with Dzyaloshinski-Moriya interaction in non-inertial frames. Results Phys. 2021;21:103759.
- [60] Indrajith VS, Sankaranarayanan R. Effect of environment on quantum correlation in Heisenberg XYZ spin model. Phys A. 2021;582:126250.
- [61] El Aroui A, Khedif Y, Habiballah N, Nassik M, Aroui AE, Khedif Y, et al. Characterizing the thermal quantum correlations in a two-qubit Heisenberg XXZ spin-chain 1/2 under Dzyaloshinskii-Moriya and Kaplan-Shekhtman-Entin-Wohlman-Aharony interactions. Opt Quantum Elec. 2022;54:694.
- [62] Yurischev MA, Haddadi S. Local quantum Fisher information and local quantum uncertainty for general X states. Phys Lett A. 2023;476:128868.
- [63] Hosseiny SM. Quantum teleportation and phase quantum estimation in a two-qubit state influenced by dipole and symmetric cross interactions. Phys Scr. 2023;98(11):115101.
- [64] Mohr PJ, Phillips WD. Dimensionless units in the SI. Metrologia. 2014;52:40.
- [65] Maziero J, Celeri LC, Serra RM, Vedral V. Classical and quantum correlations under decoherence. Phys Rev A. 2009;80:044102.
- [66] Xu J-S, Xu X-Y, Li C-F, Zhang C-J, Zou X-B, Guo G-C. Experimental investigation of classical and quantum correlations under decoherence. Nature Commun. 2010;1:7.
- [67] Tariboon J, Ntouyas SK, Agarwal P. New concepts of fractional quantum calculus and applications to impulsive fractional qdifference equations. Adv Differ Equ. 2015;2015:18.
- [68] Tuncay Gençoğlu M, Agarwal P. Use of quantum differential equations in sonic processes. App Math Nonl Sci. 2021;6(1):21–8.
- [69] El Allati A, Bukbech S, El Anouz K, El Allali Z. Entanglement versus Bell non-locality via solving the fractional Schrödinger equation using the twisting model. Chaos Solitons Fractals. 2024;179:114446.
- [70] El Anouz K, El Allati A, Metwally N, Obada AS. The efficiency of fractional channels in the Heisenberg XYZ model. Chaos Solitons Fractals. 2023;172:113581.